PNAS

Supporting Information for

Extensive N-fixation by volcanic lightning during very large explosive eruptions

Adeline Aroskay[1]*, Erwan Martin[1]*, Slimane Bekki[2], Jean-Luc Le Pennec[3], Joël Savarino[4], Abidin Temel[5], Nelida Manrique[6], Rigoberto Aguilar[6], Marco Rivera[7], Hervé Guillou[8], Hélène Balcone-Boissard[1], Océane Phelip[1], Sophie Szopa[8]

1: Institut des Sciences de la Terre de Paris (ISTeP), Sorbonne Université ; Paris, France.
2: Laboratoire Atmosphères, Observations Spatiales (LATMOS), SU/UVSQ ; France.
3: Institut de Recherche pour le Développement (IRD) & Institut Universitaire Européen de la Mer ; Plouzané, France.
4: Institut des Géosciences de l'Environnement (IGE) ; Grenoble, France.
5: Hacettepe University, Department of Geological Engineering; Ankara, Turkey.
6: Instituto Geológico Minero y Metalúrgico (INGEMMET), Observatorio Vulcanológico del INGEMMET; Arequipa, Peru.
7: Instituto Geofísico del Perú, Observatorio Vulcanológico del Sur ; Arequipa, Peru.
8: Laboratoire des Sciences du Climat et de l'Environnement (LSCE), Université Paris-Saclay ; France.

*Corresponding authors. Email: adeline.aroskay@sorbonne-universite.fr, erwan.martin@sorbonne-universite.fr the full author list here

This PDF file includes:

Supporting Information Text

Nitrate, sulphate and chlorine analyses results:

The measured concentrations of nitrate, sulphate and chlorine in the volcanic deposits are highly variable. They vary over about 4 orders of magnitude with concentrations (in µg/g of volcanic rock) ranging from about 0.8 to 4,900 ppm for NO_3^-, 0 to 21,300 ppm for SO_4^{2-}, and 0.5 to 12,300 ppm for Cl^- respectively for the Anatolian samples, and from 0.7 to 10,900 ppm, 0 to 2,250 ppm, and 0.6 to 4,250 ppm respectively for Peru samples (Supplementary Table S1). Very high levels of SO_4^{2-} and, to a lesser extent, of Cl^- are common in volcanic deposits. They are tightly associated with large eruptions whose emissions of reduced sulphur gases and halogens are oxidised ultimately into sulphates and hydrochloric acid. Their concentrations can vary greatly from one sample to another. Among other factors, they depend on volcanic emissions during the eruption, their physicochemical transformations, and their redistribution in the volcanic deposit itself during its cooling down.

The origin of nitrates

We use the relation between $\Delta^{17}O$ vs $\delta^{18}O$ and $\delta^{18}O$ vs $\delta^{15}N$ measured in nitrates (Fig.3 and Figure S3) to assess the different nitrate sources (e.g. atmospheric, biological) in our samples.

In the EM1 pool, NO3- exhibit high $\Delta^{17}O$ (up to ≈30‰) and $\delta^{18}O$ values (> 60‰) with $\delta^{15}N$ values mostly between -15‰ and 15‰. Large positive ^{17}O anomalies in NO_3^- result necessarily from NOx oxidation by O_3, which is the only known atmospheric oxidant to bear a large $\Delta^{17}O$ value (≈35‰). In the EM2 pool, NO_3^- is characterized by $\Delta^{17}O$ close to zero and small positive $\delta^{18}O$ values in the range of ≈0‰ to 10‰; EM2 $\delta^{15}N$ values are similar to those of EM1 NO_3^-. This EM2 isotopic composition is rather indicative of NO_3^- produced from NOx oxidation by oxidants carrying a $\Delta^{17}O$ ≈ 0‰, (e.g. tropospheric OH radicals), though some biological NO_3^- produced by bacterial nitrification cannot be ruled out.

Nitrates between EM1 and EM2 seem to represent mixing between atmospheric NO_3^- formed by distinct oxidation pathways with varying contributions of oxygen atoms from ozone to the overall nitrate formation. Nitrates in the EM3 pool are characterized by $\Delta^{17}O$ close to zero, with $\delta^{15}N$ values slightly higher than EM1 and EM2 and systematically negative $\delta^{18}O$ values. Such negative $\delta^{18}O$ is rather indicative of a microbial origin for these nitrates. Although the precise mechanism of microbial NO_3^- production remains unclear, it seems that two oxygen atoms come from H_2O (present-day $\delta^{18}O$ from about -15‰ to -5‰ in Anatolia waters and from about -22‰ to -8‰ in South Peru waters) and one atom from atmospheric O_2 ($\delta^{18}O$ = +23.5‰). In that case, biological nitrates are estimated to carry low or negative $\delta^{18}O$ values, ranging between about -2.2 and 4.5‰ for Anatolia and between about -6.8 and 2.5‰ for Peru. These estimates lie on the high side of our measured $\delta^{18}O$ range for EM3-nitrates.

Fig. S1.

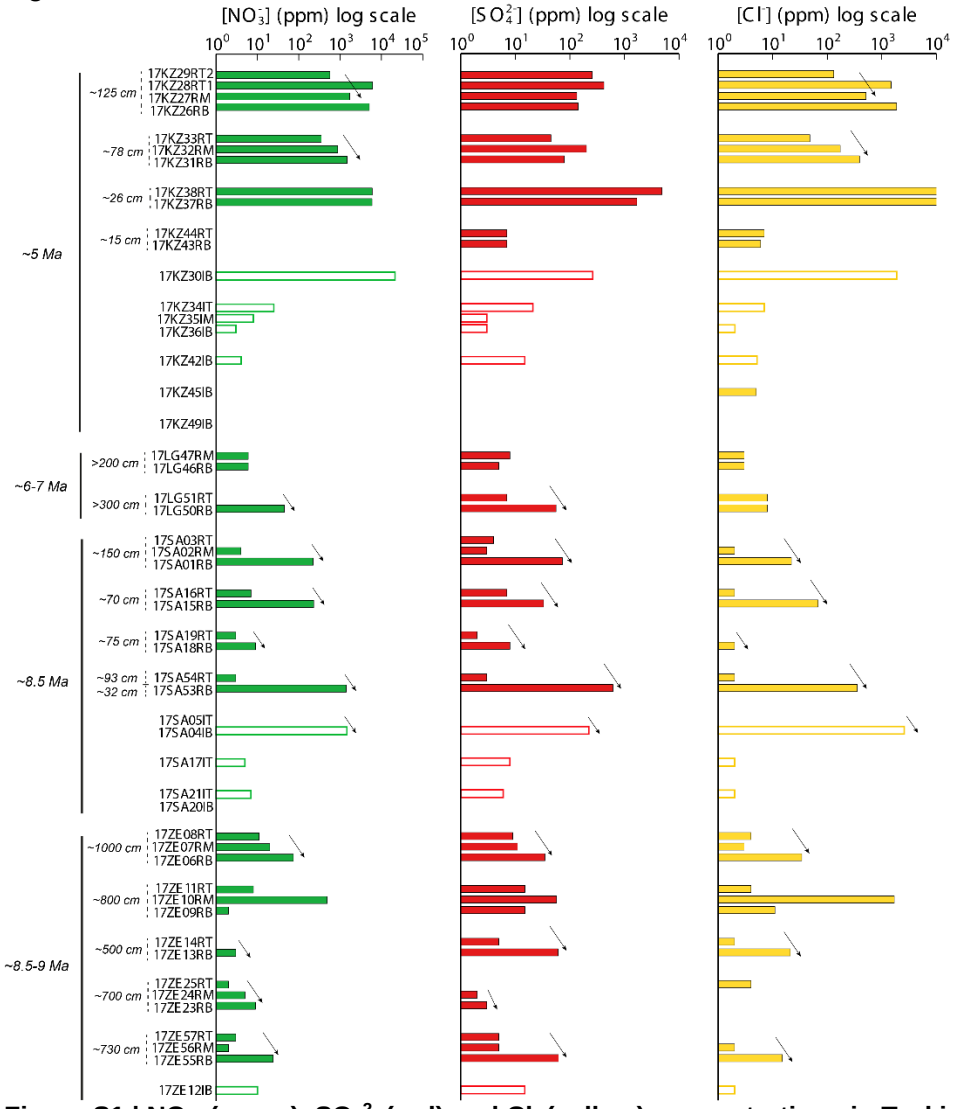

Figure S1 | NO_3^- (green), SO_4^{2-} (red) and Cl^- (yellow) concentrations in Turkish samples (n=55). Filled and empty bars represent ashfall and ignimbrite samples, respectively. Age and thickness of the deposits are indicated on the left. Type and position of the samples are indicated in their name: R stands for fallout, I stands for ignimbrite, T, M and B stand for top, middle and bottom position in the deposit, respectively. Black arrows represent the increasing concentrations from top to bottom of the deposits.

Fig. S2.

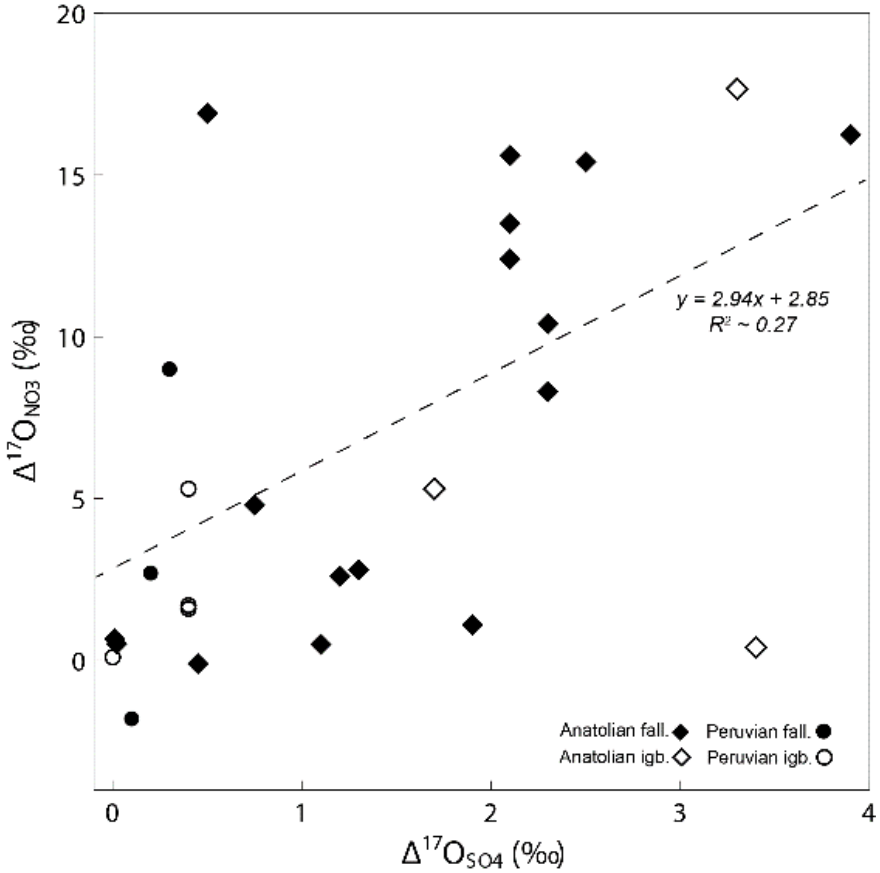

Figure S2 | $\Delta^{17}O$ in nitrates plotted against $\Delta^{17}O$ in sulphates from Anatolian (diamonds; n=20) and Peruvian (circles; n=7) volcanic deposits. $\Delta^{17}O$ is computed as $\delta^{17}O - 0.52 \times \delta^{18}O$. Filled and empty symbols represent ashfall and ignimbrite samples, respectively. The coefficient of the slope is quite consistent with the implication of ozone in the formation of nitrates and sulphates. Indeed, considering that 25% of the oxygen in sulphate molecule is inherited from ozone ($\Delta^{17}O$ ~35‰) (*7*) and that between 1/3 and 2/3 of the oxygen in nitrate is from ozone, we expect a $\Delta^{17}O_{(NO3-)}$/ $\Delta^{17}O_{(SO42-)}$ ratio between ~1.3 and ~2.7. Despite its slight correlation factor (~0.27), the $\Delta^{17}O_{(NO3-)}$/ $\Delta^{17}O_{(SO42-)}$ slope shows a coefficient ~2.9, which is quite consistent with the highest expected coefficient previously mentioned.

Fig. S3.

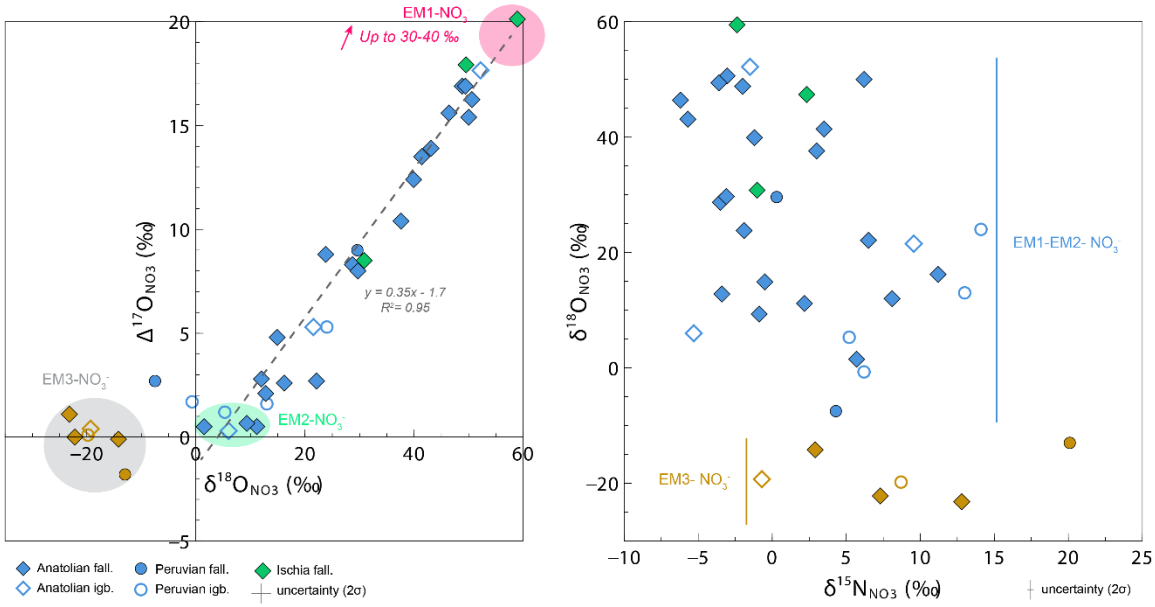

Figure S3 | $\Delta^{17}O$ vs. $\delta^{18}O$ (left) and $\delta^{18}O$ vs. $\delta^{15}N$ (right), in Anatolian (n=27), Peruvian (n=8) and Italian (n=3) volcanic deposits. Analytical uncertainties (in 2σ) are 1.5, 0.4 and 0.2 for $\delta^{18}O$, $\Delta^{17}O$ and $\delta^{15}N$, respectively. EM1 represents nitrates generated by NOx oxidation via ozone. EM2 represents atmospheric nitrates formed via the oxidation of NOx by an atmospheric oxidant with $\Delta^{17}O$=0‰ and possibly biological nitrates. Blue symbols, which are well correlated in the $\Delta^{17}O$ vs. $\delta^{18}O$ plot, correspond to nitrates with co-varying $\Delta^{17}O$-$\delta^{18}O$ isotopic compositions; they line up along with the EM1-EM2 mixing line (dotted line). EM3-NO_3^- (light brown) represent biological nitrates.

Table S1.

Samples	$[SO_4^{2-}]$	$[NO_3^-]$	$[Cl^-]$	Samples	$[SO_4^{2-}]$	$[NO_3^-]$	$[Cl^-]$
Turkey				*Peru*			
17SA01RB	73	223	22	ARE18005	16	2.9	2.7
17SA02RM	3.1	3.6	2.3	ARE18006	52	5.7	14
17SA03RT	4.4	0.6	0.5	ARE18007	45	7.7	130
17SA04IB*	222	1469	2573	ARE18008	2434	121	2714
17SA05IT*	1.4	0.6	1.0	COTA18032	0.9	0.1	1.3
17ZE06RB	35	74	34	COTA18033	29	2.5	3.5
17ZE07RM	11	20	2.6	COTA18035	12	2.2	14
17ZE08RT	9.4	11	3.7	COTA18036	1.1	0.0	1.1
17ZE09RB	15	2.3	11	COTA18039	2.0	0.2	1.5
17ZE10RM	57	486	1694	CHU18029	50	1.8	63
17ZE11RT	15	8.0	4.0	CHU18030	0.7	5.4	1.2
17ZE12IB*	15	10	2	ARE18001	27	6.3	15
17ZE13RB	61	3.2	21	ARE18002	14	1.7	4.2
17ZE14RT	5.2	0.2	1.5	ARE18003	2381	287	2181
17SA15RB	33	231	68	ARE18004	10931	2302	5711
17SA16RT	7.3	6.8	2.1	ARE18009	800	46	258
17SA17IT*	7.8	4.5	1.7	ARE18010	334	16	65
17SA18RB	8.0	9.5	2.3	ARE18011	1413	555	2015
17SA19RT	2.1	2.7	1.2	COTA18040	27	19	7.5
17SA20IB*	1.3	0.1	1.3	COTA18049	35	1848	773
17SA21IT*	6.4	7.0	1.8	ARE18012	327	112	193
17ZE23RM	1.4	1.7	1.2	ARE18013	4708	568	4245
17ZE24IB*	1118	4.6	2.3	ARE18014	1274	32	258
17ZE23RB	2.9	9.3	1.4	ARE18016	24	0.8	12
17ZE24RM	2.1	4.6	1.5	ARE18021	15	12	3.5
17ZE25RT	1.5	2.0	3.9	ARE18023	3.2	2.5	1.8
17KZ26RB	142	5090	1864	ARE18015	5.1	1.0	1.5
17KZ27RM	134	1711	514	ARE18017	189	21	788
17KZ28RT1	422	5667	1413	ARE18018	349	8.9	69
17KZ29RT2	257	538	126	ARE18020	3.6	3.6	1.6
17KZ30IB*	264	21307	1863	CHU18025	3.5	1.5	1.6
17KZ31RB	79	1478	391	CHU18026	9.2	2.8	3.9
17KZ32RM	201	875	173	CHU18027	2.5	0.1	0.8
17KZ33RT	45	351	48	CHU18031	1.3	0.1	0.6
17KZ34IT*	21	25	7.1	COTA18042	885	2248	928
17KZ35IM*	2.9	7.5	1.3	PAMP18048	52	22	25
17KZ36IB*	3.0	2.8	1.8				
17KZ37RB	1691	5933	10575				
17KZ38RT	4882	5998	12309				
17TD40LM	12	3.4	2.9				

17KZ41RW	59	1.9	11
17KZ42IB*	15	3.9	4.7
17KZ43RB	7.0	1.0	5.9
17KZ44RT	6.5	0.0	7.4
17KZ45IB*	1.2	0.9	4.9
17LG46RB	4,8	5,8	2.7
17LG47RM	8.1	6.1	2.7
17KZ49IB*	0.8	0.0	1.2
17LG50RB	56	45	8.0
17LG51RT	6.7	1.3	8.3
17SA53RB	617	1404	354
17SA54RT	2.9	2.9	1.5
17ZE55RB	62	24	15
17ZE56RM	5.1	2.2	2.3
17ZE57RT	4.9	3.2	1.3

Supplementary Table S1 | Anionic composition (sulphate, nitrate and chlorine ions) measured in Anatolian and Peruvian samples (in ppm or µg/g of rock).

Table S2.

Samples	$\delta^{18}O$	$\Delta^{17}O$	$\delta^{15}N$	Samples	$\delta^{18}O$	$\Delta^{17}O$	$\delta^{15}N$
Turkey				*Peru*			
17KZ26RB	9.3	0.7	-0.9	ARE18013	29.6	9	0.3
17KZ27RM	11.2	0.5	2.2	COTA18042*	13	1.6	13
17KZ34IT*	52.2	17.7	-1.5	ARE18004*	24	5.3	14.1
17LG53RB	50.6	16.3	-3.1	COTA18049*	5.3	1.2	5.2
17SA04IB*	21.5	5.3	9.6	ARE18008	-13	-1.7	20
17SA01RB	-23.2	1.1	12.8	ARE18009*	-19.8	0.1	8.7
17ZE06RB	41.4	13.5	3.5	ARE18010	-7.5	2.7	4.3
17ZE07RM	37.6	10.4	3	ARE18011*	-0.7	1.7	6.2
17ZE11RT	-22.2	-0.01	7.3				
17ZE12IB*	-19.3	0.4	-0.7				
17SA15RB	48.8	16.9	-2				
17SA16RT	50	15.4	6.2				
17KZ30IB*	6	0.3	-5.3				
17KZ31RB	12	2.8	8.1				
17KZ33RT	16.2	2.6	11.2				
17LG50RB	28.7	8.3	-3.5				
17LG51RT	12.8	2.1	-3.4				
17SA54RT	23.8	8.8	-1.9				
17ZE55RB	49.4	16.9	-3.6				
17ZE56RM	29.7	8	-3.1				
17ZE57RT	43.1	13.9	-5.7				
17ZE08RT	39.9	12.4	-1.2				
17KZ29RT2	-14.2	-0.1	2.9				
17KZ32RM	1.5	0.5	5.7				
17ZE13RB	14.9	4.8	-0.5				
17SA18RB	46.4	15.6	-6.2				
17ZE25RT	22.1	2.7	6.5				

Analytical uncertainties of 1.5, 0.4 and 0.2 for $\delta^{18}O$, $\Delta^{17}O$ and $\delta^{15}N$ respectively. Mean value and uncertainty in 2σ are also indicated. Asterisk indicates ignimbrite samples.

Supplementary Table S2 | Isotopic composition ($\delta^{18}O$, $\Delta^{17}O$ and $\delta^{15}N$) of nitrate from Anatolian and Peruvian samples (in ‰).

Table S3.
Considering the heterogeneity of our samples we use the average values for each deposits.

Deposit	Age (Ma)	$[NO_3^-]$ (ppm)	Minimal deposit volume (V) (km^3)	Mass of N * (Tg)	Nitrogen production (mole N)	Reference (Age and Volume)
			Turkey			
Zelve	8.5-9	40	120	2.3	1.7×10^{11}	(*8*)
Sarimaden	8.3-8.7	240	80	8.7	6.2×10^{11}	(*8*)
Kizilkaya	4.5-5.5	2700	180	218.8	1.6×10^{13}	(*8*)
			Peru			
Aeropuerto	1.65	530	19	5.4	3.9×10^{11}	(*9*)
Sencca sup	1.8-2	2	23	0.02	1.3×10^{9}	(*10*)
Sencca inf	2.8-5.1	930	62	26	1.9×10^{12}	(*10*)
La Joya	4.8	80	20	0.69	4.9×10^{10}	(*9*)
Chuquibamba	13-14	1	88	0.05	3.2×10^{9}	(*10*)
Alpabamba	18-20	1130	550	282	2×10^{13}	(*10*)

Supplementary Table S3 | Average nitrate concentration in ppm (µg/g of rock), minimal volume of deposits (km^3), estimated average mass of fixed N (Tg) and estimated average production of fixed N (mole) for each deposit.

** Mass of N = $Volume_{(deposit)}$ * density * $[NO_3^-]$*$M_{(N)}/M_{(NO3)}$*

Volume: estimated volume of each volcanic deposit (ref 8, 9 and 10)

Density: an average density for rhyolitic ignimbrite of 2000kg/m^3

$[NO_3^-]$: mean nitrate concentration in a volcanic deposit (calculated from Table S1)

$M_{(N)}$ and $M_{(NO3)}$: molar mass of nitrogen and nitrate

Table S4.

Location		Sample	$[SO_4^{2-}]$	$[NO_3^-]$	$[Cl^-]$	$\delta^{18}O_{NO3-}$	$\Delta^{17}O_{NO3-}$	$\delta^{15}N_{NO3-}$
Ischia	Tischiello eruption (~75kyrs)	015 0314 (top of the deposit)	92.3	44.5	1674.6	48	17.9	2.4
		015 0309 (bottom of the deposit)	925.8	450	17576.1	31.4	8.4	-1
	Monte Epemeo Green Tuff eruption (~55kyrs)	015 0321 (bottom of the deposit)	1251.5	76.9	2492.7	58.7	20.6	-2.4

Supplementary Table S4 | Anionic (sulphate, nitrate and chlorine ions) concentration (in ppm) and isotopic ($\delta^{18}O$, $\Delta^{17}O$ and $\delta^{15}N$) compositions of nitrate (in ‰) from Ischia samples.

SI References

1. E. Le Gendre, E. Martin, B. Villemant, P. Cartigny, N. Assayag, A simple and reliable anion-exchange resin method for sulfate extraction and purification suitable for multiple O- and S-isotope measurements. *Commun. mass Spectrom.*, 137–144 (2016).
2. H. Bao, M. H. Thiemens, Generation of O 2 from BaSO 4 Using a CO 2 −Laser Fluorination System for Simultaneous Analysis of δ 18 O and δ 17 O. *Anal. Chem.* **72**, 4029–4032 (2000).
3. S. Morin, thesis (2008).
4. H. Bao, X. Cao, J. A. Hayles, Triple Oxygen Isotopes: Fundamental Relationships and Applications. *Annu. Rev. Earth Planet. Sci.* **44**, 463–492 (2016).
5. S. Morin, J. Savarino, S. Bekki, S. Gong, J. W. Bottenheim, E. Canada, Signature of Arctic surface ozone depletion events in the isotope anomaly (17 O) of atmospheric nitrate. *Atmos. Chem. Phys.*, 1451–1469 (2007).
6. S. S. Cliff, M. H. Thlemens, High-Precision Isotopic Determination of the 18O/16O and 17O/16O ratios in nitrous oxide. *Anal. Chem.*, 2791–2793 (1994).
7. J. Savarino, C. C. W. Lee, M. H. Thiemens, Laboratory oxygen isotopic study of sulfur (IV) oxidation: Origin of the mass-independent oxygen isotopic anomaly in atmospheric sulfates and sulfate mineral deposits on Earth. *J. Geophys. Res.* **105** (2000).
8. J.-L. Le Pennec, J.-L. Bourdier, J.-L. Froger, A. Temel, G. Camus, A. Gourgaud, Neogene ignimbrites of the Nevsehir plateau (central Turkey)" stratigraphy, distribution and source constraints. *J. Volcanol. Geotherm. Res.* **63**, 59–87 (1994).
9. P. Paquereau, J. Thouret, G. Wörner, M. Fornari, Neogene and Quaternary ignimbrites in the area of Arequipa , Southern Peru : Stratigraphical and petrological correlations. *J. Volcanol. Geotherm. Res.* **154**, 251–275 (2006).
10. J.-C. Thouret, B. R. Jicha, J.-L. Paquette, E. H. Cubukcu, A 25 myr chronostratigraphy of ignimbrites in south Peru: implications for the volcanic history of the Central Andes. *J. Geol. Soc. London.* **173**, 734–756 (2016).